

Data-driven sparse polynomial chaos expansion for models with dependent inputs

Zhanlin Liu¹, Youngjun Choe¹

Abstract

Polynomial chaos expansions (PCEs) have been used in many real-world engineering applications to quantify how the uncertainty of an output is propagated from inputs. PCEs for models with independent inputs have been extensively explored in the literature. Recently, different approaches have been proposed for models with dependent inputs to expand the use of PCEs to more real-world applications. Typical approaches include building PCEs based on the Gram-Schmidt algorithm or transforming the dependent inputs into independent inputs. However, the two approaches have their limitations regarding computational efficiency and additional assumptions about the input distributions, respectively. In this paper, we propose a data-driven approach to build sparse PCEs for models with dependent inputs. The proposed algorithm recursively constructs orthonormal polynomials using a set of monomials based on their correlations with the output. The proposed algorithm on building sparse PCEs not only reduces the number of minimally required observations but also improves the numerical stability and computational efficiency. Four numerical examples are implemented to validate the proposed algorithm.

Keywords: uncertainty quantification, polynomial chaos expansion, sparse polynomial chaos expansion, Gram-Schmidt orthogonalization

1. Introduction

Uncertainty quantification plays a critical role in many domains of real-world engineering applications as it characterizes the uncertainties of the system

outputs in those applications. Surrogate models often serve as mathematical models to describe how the uncertainty of a system output is propagated from the inputs. Among the surrogate models, polynomial chaos expansions (PCEs) have been widely used to conduct the uncertainty quantification on the outputs in many industrial applications including thermodynamics [1], electromagnetism [2], chemical engineering [3], aerodynamics [4], , hydrogeology [5], structural safety analysis [6, 7], power systems [8], and manufacturing [9, 10].

To accurately conduct uncertainty quantification for models with different types of inputs, a variety of PCEs have been developed in the literature. For models with independent inputs, the Wiener chaos expansion, which is known as the first PCE in the literature, uses Hermite polynomials to construct PCE models for Gaussian-distributed inputs [11]. Later PCEs, including the generalized PCE (gPCE) [12], the multi-element gPCE (ME-gPCE) [13], the moment-based arbitrary PCE (aPCE) [14], the support vector regression based PCE [15], and the Gram-Schmidt based PCE (GS-PCE) [16], are developed for independent inputs following non-Gaussian distributions.

Even though the GS-PCE can also be used to construct PCEs for models with dependent inputs, the procedure of using Gram-Schmidt algorithm is computationally demanding as the number of the inputs increases or the expansion order increases [17]. Therefore, [17] provides an alternative method to construct PCE for models with dependent inputs by transforming the dependent inputs into independent inputs using the Rosenblatt transformation. However, this approach might not be applicable to many engineering applications due to the fact that the Rosenblatt transformation requires the knowledge about the conditional probability density functions about the inputs, which is often not the case in practice. Thus, how to efficiently construct a PCE for models with dependent inputs without using distribution information about the inputs still requires more investigations.

Consequently, the main contribution of this paper is to propose a sparse PCE algorithm which can efficiently construct sparse PCEs for models with both independent or dependent inputs regardless of the input distribution. To the best

of our knowledge, the proposed method is also the first data-driven method that constructs a sparse PCE for models with dependent inputs without requiring a large number of observations. We validate the proposed method empirically using four simulation examples by estimating the variance of the output and the Kullback-Leibler (KL) divergence from the estimated output distribution to the true distribution. The simulation examples show the advantage of the proposed method in terms of computational speed and numerical stability of constructing orthogonal polynomials [17]. In addition, the proposed method is more accurate on estimating the lower-order moments and distribution of the output comparing with the state-of-the-art method on constructing sparse PCE models regardless of the input distribution and their dependency structure.

The remainder of this paper is organized as follows. Sec. 2 briefly reviews the technical background on the PCE and the state-of-the-art methods on constructing sparse PCEs. Sec. 3 proposes the algorithm of the proposed method and discusses the advantages of using the proposed method. In Sec. 4, the proposed algorithm is empirically evaluated using four simulation examples. Sec. 5 concludes the paper with a discussion on future research directions.

2. Background

In this section, we will first introduce PCE models and how to estimate the lower-order moments using the PCE model coefficients. Then we will review how to construct GS-PCE since it is regarded as the pioneering work of data-driven PCE model regardless of the distribution and dependency of the inputs. In the end, we will review the state-of-the-art routine for constructing sparse PCEs for dependent inputs, which applies the least angle regression method on orthonormal polynomials constructed using the modified Gram-Schmidt algorithm.

2.1. PCE model

PCE models the relationship between the n random inputs in \mathbf{X} and the output Y using a finite number of orthonormal polynomials as follows:

$$Y = f(\mathbf{X}) \approx \sum_{i=0}^P \theta_i \psi_i(\mathbf{X}), \quad (1)$$

where θ_i , $i = 0, 1, 2, \dots, P$, are called PCE coefficients and ψ_i , $i = 1, 2, \dots, P$ are orthonormal polynomials. The orthonormal polynomials can be constructed based on different PCE models. We will particularly introduce how to construct orthonormal polynomials using the modified Gram-Schmidt algorithm in Section 2.2.

$$P + 1 = \binom{n + p}{n} \quad (2)$$

is the number of polynomial terms, where p is the highest polynomial degree in the PCE model. As p increases to infinity, the error of estimating the output using the PCE model converges to 0 [18].

In this paper, the PCE coefficients are solved by solving an overdetermined linear system equations in the least-squares sense using a regression as follows [19]:

$$\operatorname{argmin}_{\boldsymbol{\theta} \in \mathbb{R}^{P+1}} \sum_{j=1}^m \left(Y_j - \sum_{i=0}^P \theta_i \psi_i(\mathbf{X}_j) \right)^2, \quad (3)$$

where $\boldsymbol{\theta}$ denotes $(\theta_0, \theta_1, \dots, \theta_P)$. Y_j and \mathbf{X}_j represent the output and the input vector of the j^{th} observation, $j = 1, \dots, m$, respectively.

Thanks to the orthogonality of the orthonormal polynomials, we can approximate the lower-order moments of output Y using the PCE coefficients as follows:

$$\begin{aligned} \mathbb{E}(Y) &\approx \theta_0, \\ \operatorname{Var}(Y) &\approx \sum_{i=1}^P \theta_i^2. \end{aligned} \quad (4)$$

The accuracy of estimating the lower-order moments improves as P in Eq. (4) increases.

2.2. GS-PCE

The GS-PCE constructs orthonormal polynomials based on P initial polynomials $(e_i)_{i \in \{1, 2, \dots, P\}}$, where $e_i, i = 1, 2, \dots, P$, are assumed to be linearly independent. Then the orthonormal polynomials $(\psi_i(\mathbf{X}))_{i \in \{1, 2, \dots, P\}}$ are obtained using the modified Gram-Schmidt algorithm described as follows [20]:

Algorithm 1 Modified Gram-Schmidt Algorithm

Require: P linearly independent initial polynomials $(e_i)_{i \in \{1, 2, \dots, P\}}$.

Ensure: P orthonormal polynomials $(\psi_i(\mathbf{X}))_{i \in \{1, 2, \dots, P\}}$.

- 1: **for** $i = 1, 2, \dots, P$ **do**
 - 2: $\phi_i(\mathbf{X}) \leftarrow e_i(\mathbf{X})$
 - 3: **for** $k = 1, 2, \dots, i - 1$ **do**
 - 4: $\phi_i(\mathbf{X}) \leftarrow \phi_i(\mathbf{X}) - \langle \phi_i(\mathbf{X}), \psi_k(\mathbf{X}) \rangle \psi_k(\mathbf{X})$
 - 5: **end for**
 - 6: $\psi_i(\mathbf{X}) \leftarrow \frac{\phi_i(\mathbf{X})}{\|\phi_i(\mathbf{X})\|_2}$
 - 7: **end for**
-

The inner-product in the algorithm is defined with respect to the empirical measure in this paper.

Even though GS-PCE provides feasibility on constructing orthonormal polynomials for dependent inputs following arbitrary distributions, it is computationally demanding as the number of input or polynomial order increases [17]. In addition, the GS-PCE might be inaccurate for models with highly correlated inputs since the constructed orthonormal polynomials might lose their orthogonality due to the rounding error [21].

2.3. Sparse PCE

A variety of sparse PCEs have been explored in the literature. [22] proposes a greedy forward-backward selection algorithm, which is regarded as a pioneering work for constructing sparse PCEs in the literature. Based on this work, many other techniques have been introduced to construct sparse PCEs using the least angle regression (LAR) and the diffeomorphic modulation under

observable response preserving homotopy (D-MORPH) regression [23] as well as solving a sparse regression with a regularization term [24, 25, 26]. These techniques can also be applied to construct sparse PCEs with m orthonormal polynomials using the algorithm summarized in Algorithm 2. Even though there also exist other methods for constructing sparse PCEs without using the Gram-Schmidt algorithm [27, 28, 26, 29], they require assumptions on the dependency or distributions of the inputs.

Algorithm 2 Sparse PCE algorithm for models with dependent inputs

Require: At least $P + 1$ random observations of output Y and inputs \mathbf{X} .

Ensure: A sparse PCE representation of Y with respect to $\{\psi_{i'}(\mathbf{X})\}_{i'=1}^m$.

- 1: Construct P initial linearly independent polynomials $(e_i)_{i \in \{1, 2, \dots, P\}}$.
 - 2: Construct orthonormal polynomial basis $\{\psi_i(\mathbf{X})\}_{i=1}^P$ using the modified Gram-Schmidt polynomials described in Algorithm 1.
 - 3: Construct a sparse PCE model of Y by selecting $\{\psi_{i'}(\mathbf{X})\}_{i'=1}^m \subseteq \{\psi_i(\mathbf{X})\}_{i=1}^P$ based on a sparse regression.
-

As the procedure of the modified Gram-Schmidt algorithm is embedded in Algorithm 2, it inherits the computational inefficiency and inaccuracy from Algorithm 1. To address these drawbacks, we propose an algorithm in the following section that improves the efficiency and accuracy of constructing a sparse PCE for a model with dependent inputs. Step 3 in Algorithm 2 can use any sparse regression method. In this paper, as the benchmark method for empirical validation in Section 4, we use the LAR-based method to build sparse PCEs.

3. Methodology

As we described in Section 2.2, constructing orthonormal polynomials becomes more computationally demanding as the number of inputs or polynomial order increases. Therefore, we propose a new algorithm which builds a sparse PCE regardless of the distributions and dependency structure of the inputs.

The proposed algorithm not only removes the need for a large number of random observations but also improves the estimation accuracy and computational speed.

Unlike the benchmark method described in Algorithm 2, which constructs P orthonormal polynomials based on P initial linearly independent polynomials before applying an operator to construct a sparse PCE, the proposed algorithm only constructs a limited number of orthonormal polynomials that significantly explain the output Y from P initial polynomials.

The proposed sparse PCE algorithm is a recursive algorithm which requires a pre-defined threshold value $\epsilon \in (0, 1)$ and a set of initial polynomials $\{e_i^{(0)}\}_{i \in \{1, 2, \dots, P^{(0)}\}}$ at its initial step, where $l = 0$ represents the iteration counter. As it is defined in Eq. (2), $P^{(0)}$, which is the number of the initial polynomials, depends on the number of inputs n and the polynomial order p . In this paper, the $P^{(0)}$ initial polynomials are constructed by the tensor product of the univariate polynomial of each input X_i in \mathbf{X} , $i = 1, 2, \dots, n$ as follows:

$$\{e_i^{(0)}\}_{i \in \{1, 2, \dots, P^{(0)}\}} = \left\{ \prod_{k=1}^n X_k^{j_k} : j_k \in \{0, 1, \dots, p\}, \sum_{k=1}^n j_k \leq p \right\}. \quad (5)$$

In the l^{th} iteration, we calculate $\forall i \in \{1, 2, \dots, P^{(l-1)}\}, \rho(e_i^{(l-1)}(\mathbf{X}), Y)$, where $\rho(\cdot, \cdot)$ is an operator that calculates the empirical Pearson correlation coefficient between two variables. The algorithm stops with the following condition:

$$\forall i \in \{1, 2, \dots, P^{(l-1)}\}, \rho(e_i^{(l-1)}(\mathbf{X}), Y) < \epsilon. \quad (6)$$

Otherwise, we create $\{e_i^{(l)}\}_{i \in \{1, 2, \dots, P^{(l)}\}}$ by keeping *only* $e_i^{(l-1)}(\mathbf{X})$ that satisfies the condition

$$\rho(e_i^{(l-1)}(\mathbf{X}), Y) \geq \epsilon, \forall i \in \{1, 2, \dots, P^{(l-1)}\}. \quad (7)$$

This procedure prevents selecting polynomials that are linearly dependent or highly correlated with the constructed orthonormal polynomials in the previous iterations and reduces the number of constructed orthonormal polynomials compared with the modified Gram-Schmidt algorithm. In the next step, we se-

lect one polynomial ($e_i^{(l)}(\mathbf{X}) \in \{e_i^{(l)}\}_{i \in \{1, 2, \dots, P^{(l)}\}}$), which satisfies the equation as follows:

$$\forall j \in \{1, 2, \dots, P^{(l)}\}, \rho(e_i^{(l)}(\mathbf{X}), Y) \geq \rho(e_j^{(l)}(\mathbf{X}), Y). \quad (8)$$

After we get $e_i^{(l)}(\mathbf{X})$, we transform it into an orthonormal polynomial with respect to $\{\psi_i(\mathbf{X})\}_{i=1}^{l-1}$ using Steps 2–6 in Algorithm 1. Unlike the modified Gram-Schmidt algorithm, which constructs orthonormal polynomials based on the initial polynomials whose ordering is defined, the proposed algorithm constructs the orthonormal polynomials based on their correlations with Y . To be more specific, the polynomials which have high correlations with Y are selected first to construct the orthonormal polynomials. It is shown that such ordering improves the numerical stability of constructing orthonormal polynomials in Section 4. The proposed algorithm is summarized in Algorithm 3.

Algorithm 3 Forward-selection sparse PCE (FSS-PCE) algorithm

Require: Random observations of output Y and inputs \mathbf{X} ; Threshold value ϵ ;

Iteration counter $l = 0$.

Ensure: A sparse PCE representation of Y with respect to $\{\psi_i(\mathbf{X})\}_{i=0}^l$.

- 1: Construct P initial polynomials $\{e_i^{(l)}\}_{i \in \{1, 2, \dots, P^{(l)}\}}$ using Eq. (5).
 - 2: Increase l by 1 and select $e_l(\mathbf{X}) \in \{e_i^{(l-1)}\}_{i \in \{1, 2, \dots, P^{(l-1)}\}}$ based on Eq. (8).
 - 3: Update $\{e_i^{(l)}\}_{i \in \{1, 2, \dots, P^{(l+1)}\}}$ based on Eq. (7).
 - 4: Transform $e_l(\mathbf{X})$ into $\psi_l(\mathbf{X})$ using Steps 3–6 in Algorithm 1, where $e_l(\mathbf{X})$ and $\{\psi_i(\mathbf{X})\}_{i=0}^{l-1}$ replace $\phi_i(\mathbf{X})$ and $\{\psi_k(\mathbf{X})\}_{k=1}^{i-1}$, respectively.
 - 5: Check Eq. (6) and if satisfied, go to step 6. Otherwise, go to Step 2.
 - 6: Model the output Y using a sparse PCE model with respect to $\{\psi_i(\mathbf{X})\}_{i=1}^l$ using Eq. (1).
-

The pre-specified ϵ decides the goodness of fitting and the sparseness of the PCE model. It is chosen by conducting an K -fold cross-validation. To conduct the K -fold cross-validation, we first randomly split all random observations into K subsets where each subset contains the same number of observations. Then we treat each subset as a testing set and the rest of the subsets as a training

set. After that, we construct a sparse PCE using Algorithm 3 and estimate PCE coefficients of a sparse PCE based on the training set and predict Y on the testing set using its inputs. By following this procedure for K times, where each time we use a different subset as the testing set, we choose ϵ based on the optimization as follows:

$$\operatorname{argmin}_{\epsilon \in (0,1)} \sum_{j=1}^n \left(\mathbf{Y}_j - \sum_{i=0}^{P^{(j)}} \theta_{i,\epsilon}^{(j)} \psi_{i,\epsilon}^{(j)}(\mathbf{X}_j) \right)^2, \quad (9)$$

where \mathbf{Y}_j represents the outputs in the j^{th} fold. $\{\psi_i^{(j)}(\mathbf{X}_j)\}_{i=0}^{P^{(j)}}$ and $\boldsymbol{\theta}^{(j)}$ are the orthonormal polynomials and the PCE coefficients estimated based on the rest of the folds, respectively.

4. Empirical validation

In this section, we present four numerical examples to empirically validate the proposed method. The first and second examples consider the inputs that are independent and dependent, respectively, in synthetic settings. The third and fourth examples consider modeling the output using sparse PCE for dependent inputs in real-world problems.

In this paper, we use the relative error (RE) to compare the accuracy of estimating the standard deviation of Y for both the benchmark method and the proposed method. The relative error is defined as follows:

$$\epsilon_{re} = \frac{|\sigma_Y - \hat{\sigma}_Y|}{\sigma_Y}, \quad (10)$$

where σ_Y is the theoretical standard deviation of Y or an estimate using the Monte Carlo method based on a large number of random observations. $\hat{\sigma}_Y$ is the estimated standard deviation of Y using either the benchmark method or the proposed method using Eq. (4). In each simulation example, a smaller ϵ_{re} represents a more accurate estimation. Note that the accurate estimation of σ_Y using all the PCE coefficients in Eq. (4) indicates that the PCE represents an accurate spectral decomposition of the uncertainty in Y with respect to \mathbf{X} .

Thus, the PCE is useful for uncertainty quantification such as the variance-based sensitivity analysis, which aims to quantify the influence of each input on the output variance [20].

In addition, we also compare the goodness of fit of two methods by estimating the KL divergence from the estimated output distribution to the true distribution [30]. Note that the relative error ϵ_{re} evaluates how well the two methods estimate the *second-order moment* of Y (which is important for sensitivity analyses in practice), whereas the KL divergence evaluates how well the methods approximate the *overall distribution* of Y . These two metrics are also used to evaluate PCE models in [17].

4.1. Ishigami function approximation

We use the Ishigami function [31] in Eq. (11) as our first simulation example to validate the proposed method for a model with *independent* inputs.

$$Y = \sin(X_1) + 7 \sin^2(X_2) + 0.1X_3^4 \sin(X_1), \quad (11)$$

where $X_i \sim \mathcal{U}(-\pi, \pi), i = 1, 2, 3$. This function is widely used as a test function to benchmark PCE methods due to its strong non-linearity and non-monotonicity [17].

In this example, we first show how to choose the threshold value for the proposed method. In addition, we compare the proposed method with the benchmark method in Section 2.3 in terms of the estimation accuracy and computational efficiency.

The 5-fold cross-validation is used to find the optimal threshold value for the proposed method considering different polynomial orders using 200 random observations. The blue (resp. red) points of the left subfigure and right subfigure in Figure 1 represent the threshold values that correspond to the minimal cross-validation errors as defined in Eq. (9) for the PCE with the polynomial order of 3 (resp. 4) and 8 (resp. 9), respectively. In addition, as it is presented in Figure 1, the proposed model with a higher polynomial order achieves a smaller cross-validation error than the model with a lower polynomial order. It reflects

the fact that a more complex PCE model tends to better approximate a target function.

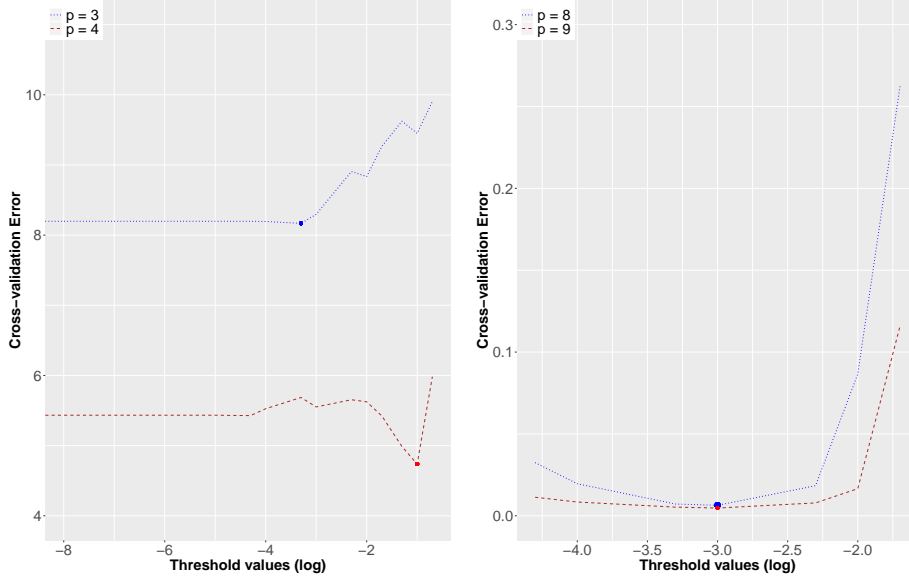


Figure 1: The left subgraph shows the 5-fold cross-validation errors of PCEs with $p = 3$ and $p = 4$ across different threshold values for the proposed method. The right subgraph shows the 5-fold cross-validation errors of PCEs with $p = 8$ or $p = 9$ across different threshold values. The blue (resp. red) points represent the threshold values that correspond to the threshold values in Eq. (9) for PCEs with $p = 3$ (resp. 4) or $p = 8$ (resp. 9).

We first compare how the polynomial order p and the sample size m interactively affect the performance for both the benchmark method and the proposed method. The left subfigure in Figure 2 shows that the proposed method achieves a better accuracy by increasing the polynomial order when the sample size is small. On the other hand, the performance of the benchmark method does not improve as the polynomial order increases when the polynomial order is greater than 6. This is due to the numerical instability by the over-parametrization of using the GS-PCE based on an insufficient number of random observations. The right subfigure in Figure 2 shows the trend that increasing the polynomial order improves the accuracy for both methods given a large sample size. Therefore, we conclude that the proposed method achieves the similar or a better accuracy

than the benchmark method given the same number of observations for models with independent inputs.

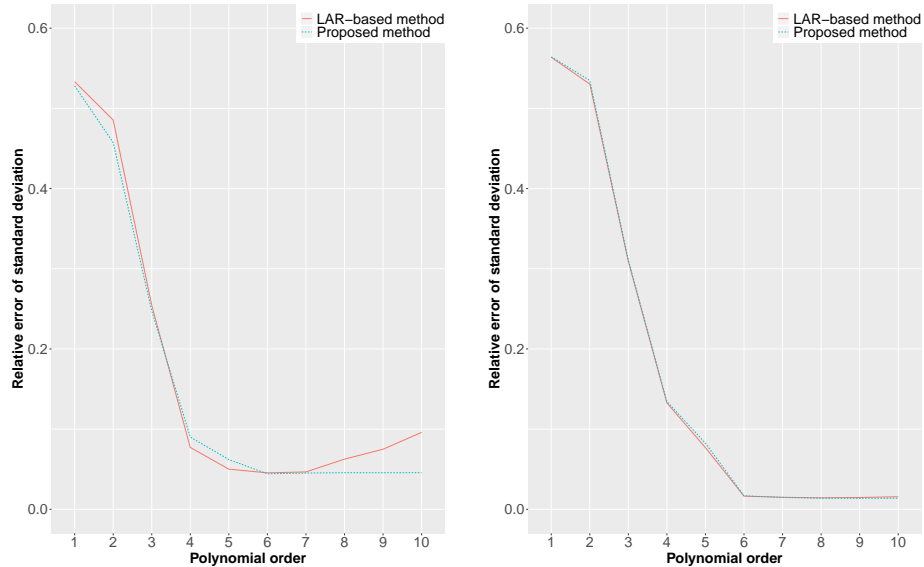


Figure 2: The plots show the relative errors of estimating the standard deviation of Y using $m = 100$ (left) and 1000 (right) random observations for both methods. The relative error is averaged across 50 simulation runs for each polynomial order p .

Furthermore, we study how the sample size m affects the estimation accuracy of the proposed method compared with the benchmark method based on a fixed polynomial order $p = 8$. As shown in Figure 3, the proposed method achieves a much better accuracy than the benchmark method when the sample size is small. When the sample size is large, both methods perform similarly as expected. Besides comparing the estimation accuracy of the standard deviation, we also compare the model performance by estimating the KL divergence using two different methods on different sample sizes. When the sample size is 1000, the mean and standard error of the KL divergence for the proposed method and the benchmark method are $-0.0031 (\pm 0.0003)$ and $0.0057 (\pm 0.0004)$ based on 50 simulation runs, respectively. When the sample size is 100, the mean and standard error of the KL divergence using the proposed method is $0.005 (\pm 0.001)$. It is much smaller than the KL divergence of using the benchmark

method 0.055 (± 0.003). This also validates that the proposed method has a better computational accuracy than the benchmark method.

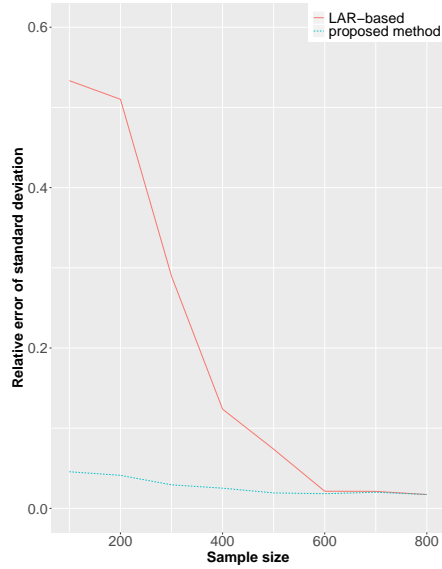


Figure 3: Relative errors of estimating the output standard deviation with $p = 8$ v.s. the number of random observations. The relative errors are averaged across 50 simulation runs for each sample size.

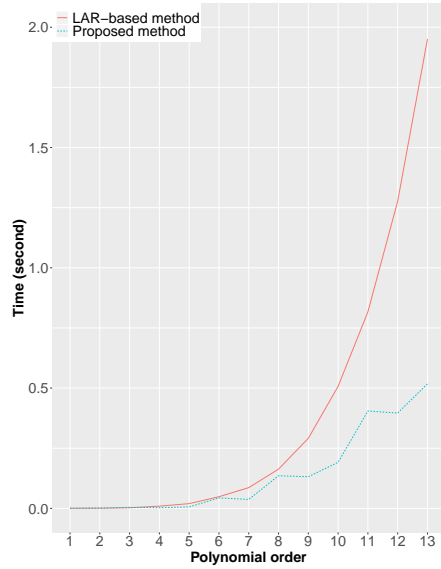


Figure 4: Computational time (seconds) v.s. the polynomial order p for both methods. For each polynomial order, the computational time is averaged across 50 simulation runs, where each simulation run uses 1,000 random observations.

In addition, we compare the computational efficiency of the proposed method with the benchmark method in terms of the computational time. The computational times are recorded using a 1.4 GHz Intel Core i5 machine with a 16 GB 1600 MHz DDR3 RAM. The average computation times for both methods are calculated based on 50 simulation runs for the polynomial order of $p = 1$ through $p = 13$ using 1,000 random observations in each simulation run. As shown in Figure 4, the computational time for the benchmark method increases exponentially as the polynomial order increases. It can be explained by Eq. (2) since the number of constructed orthonormal polynomials increases exponentially as the polynomial order p increases. However, the computation time for

the proposed method grows much more slowly. This can be intuitively explained by Step 2 in Algorithm 3 since the number of polynomials is reduced in each iteration.

4.2. Numerical example with dependent inputs

We use a numerical example in [20] as our second example to validate the proposed method for models with dependent inputs. This example involves multiple types of probability distributions of inputs as follows:

$$\begin{aligned}
 \begin{pmatrix} X_1 \\ X_2 \\ X_3 \\ X_4 \end{pmatrix} &\sim \mathcal{N} \left[\begin{pmatrix} 0 \\ 0 \\ 0 \\ 0 \end{pmatrix}, \begin{pmatrix} 1 & 0 & 0 & 0 \\ 0 & 1 & 0 & 0 \\ 0 & 0 & 1 & 0.3 \\ 0 & 0 & 0.3 & 1 \end{pmatrix} \right], \\
 X &\sim \mathcal{U}(0, 1), \\
 X_5 &= \theta_1 X + \mathcal{U}(0, 1), \\
 X_6 &= \theta_2 X + \theta_3 X^2 + \mathcal{U}(0, 1), \\
 Y &= X_1 X_2 + X_3 X_4 + X_5 X_6.
 \end{aligned} \tag{12}$$

Here, we set $(\theta_1, \theta_2, \theta_3) = (0.4, 0.6, 1)$ as in [20]. We also compare the estimation accuracy of the standard deviation of Y using the two methods. Unlike the first example, where it requires a PCE model with a large p to model the response function, this example uses a PCE model with $p = 2$ for both methods. We measure the performance of each method using $m = 20$ and $m = 100$ and report the results based on 50 replications. As it is shown in Table 1, the proposed method achieves the same accuracy as the benchmark method when $m = 100$. However, the proposed method provides a much better accuracy than the benchmark method when $m = 20$. In addition, as it is shown in Table 1 the estimated KL divergence of using the benchmark method is infinity when $m = 20$. It shows that the benchmark method cannot model the input-output relationship. However, the small KL divergence of using the proposed method indicates the robustness of the proposed method. When $m = 100$, the

proposed method still shows a better estimation of the output distribution than the benchmark method.

Table 1: Estimations of the output standard deviation and KL divergence using the benchmark method and the proposed method across 50 simulation runs. Each simulation run uses $m = 20$ or $m = 100$. The relative errors are calculated based on the theoretical value $\sigma_Y = 1.655$ provided in [20]. The estimation accuracy of the proposed method is better than the benchmark method when $m = 20$. The KL divergence of the proposed method is smaller than the benchmark method for both sample sizes.

Sample size	Method	Estimation	Relative error	KL divergence
20	Benchmark method	0.914 ± 0.112	44.77%	∞
	Proposed method	1.618 ± 0.051	2.23%	0.087 ± 0.013
100	Benchmark method	1.643 ± 0.027	0.73%	0.016 ± 0.002
	Proposed method	1.643 ± 0.027	0.73%	0.007 ± 0.001

4.3. 23-bar horizontal truss

We consider the 23-bar horizontal truss example in [17] as our third example. The downward vertical displacement at the mid span of the structure, Y , is considered as the output of interest. As depicted in Figure 5, the uncertainty of Y is affected by Young modulus $E_i, i = 1, 2$, cross-sectional area $A_i, i = 1, 2$ for horizontal and diagonal bars, and the random loads $P_i, i = 1, 2, \dots, 6$. All inputs in this example have the same distributions as in [17]. $E_i, i = 1, 2$ and $A_j, j = 1, 2$ are assumed to be mutually independent inputs and following the lognormal distribution with mean μ and standard deviation σ as follows:

$$\begin{aligned}
 E_1, E_2 &\sim \mathcal{LN}(2.1 \times 10^{11}, 2.1 \times 10^{10}) \text{ [Pa]}, \\
 A_1 &\sim \mathcal{LN}(2.0 \times 10^{-3}, 2.0 \times 10^{-4}) \text{ [m}^2\text{]}, \\
 A_2 &\sim \mathcal{LN}(1.0 \times 10^{-3}, 1.0 \times 10^{-4}) \text{ [m}^2\text{]}.
 \end{aligned} \tag{13}$$

Unlike $E_i, i = 1, 2$ and $A_i, i = 1, 2$ which are mutually independent, $P_i, i = 1, 2, \dots, 6$ are mutually dependent on each other. In addition, P_i marginally follows a Gumbel distribution with mean $\mu = 5 \times 10^4$ [N] and standard deviation $\sigma = 7.5 \times 10^3$ [N] with the marginal cumulative distribution function as follows:

$$F_i(x; \alpha, \beta) = e^{-e^{-(x-\alpha)/\beta}}, i = 1, 2, \dots, 6, \tag{14}$$

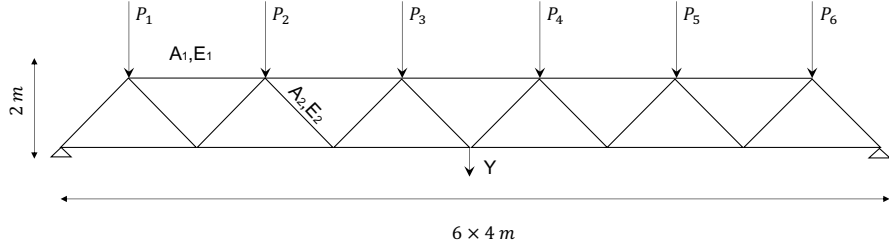


Figure 5: Schema of the horizontal truss model modified from [20]. Young modulus $E_i, i = 1, 2$, cross-sectional area $A_i, i = 1, 2$ for horizontal and diagonal bars, and the random loads $P_i, i = 1, 2, \dots, 6$ are the inputs which affect the downward vertical displacement at the mid span of the structure, Y .

where $\beta = \sqrt{6}\sigma/\pi$, $\alpha = \mu - \gamma\beta$, and $\gamma \approx 0.5772$ is the Euler-Mascheroni constant. The dependency among $P_i, i = 1, 2, \dots, 6$ is encoded using the C-vine copula with the density as follows:

$$c_{\mathbf{X}}^{(\mathcal{G})}(u_1, \dots, u_6) = \prod_{j=2}^6 c_{1j; \theta=1.1}^{(\mathcal{GH})}(u_1, u_j), \quad (15)$$

where $c_{1j; \theta=1.1}^{(\mathcal{GH})}$ is the density of the pair-copula between P_1 and $P_j, j = 2, \dots, d$. \mathcal{GH} represents the Gumbel-Hougaard family whose bivariate copula can be represented as follows:

$$C_{\theta}^{(\mathcal{GH})}(u, v) = \exp\left(-\left((-\log u)^{\theta} + (-\log v)^{\theta}\right)^{1/\theta}\right), \quad \theta \in [1, \infty),$$

where θ decides the correlations among the loads. Based on Eq. (15), we can see that P_1 is equally correlated with all the other loads. Y is simulated based on a regression of the standardized inputs with coefficients provided in [32] as

follows:

$$\begin{aligned}
Y = & 2.8070 + 1.2598E'_1 + 0.2147E'_2 + 1.2559A'_1 + 0.2133A'_2 - 0.1510P'_1 - 0.4238P'_2 - \\
& 0.6100P'_3 - 0.6100P'_4 - 0.4238P'_5 - 0.1510P'_6 - 0.1978E_1'^2 - 0.0362E_2'^2 - 0.2016A_1'^2 - \\
& 0.0346A_2'^2 + 0.0023P_1'^2 + 0.0008P_2'^2 + 0.0036P_3'^2 + 0.0036P_4'^2 + 0.0008P_5'^2 + 0.0023P_6'^2 - \\
& 0.0042E_1'E_2' - 0.3022E_1'A_1' - 0.0110E_1'A_2' + 0.0381E_1'P_1' + 0.0871E_1'P_2' + 0.1232E_1'P_3' + \\
& 0.1232E_1'P_4' + 0.0871E_1'P_5' + 0.0346E_1'P_6' + 0.0041E_2'A_1' + 0.0110A_1'A_2' + 0.0261A_1'P_1' + \\
& 0.0831A_1'P_2' + 0.1172A_1'P_3' + 0.1172A_1'P_4' + 0.0832A_1'P_5' + 0.0296A_1'P_6',
\end{aligned} \tag{16}$$

where $E'_i, i = 1, 2$, $A'_i, i = 1, 2$, and $P'_i, i = 1, 2, 3, 4, 5, 6$ are the standardized inputs. For example, $E'_1 = \frac{E - \mu_{E_1}}{\sigma_{E_1}}$, where μ_{E_1} is the mean of E_1 and σ_{E_1} is the standard deviation of E_1 .

We evaluate the benchmark method and the proposed method by averaging their performances over 50 simulation runs, where each simulation run uses $m = 20$ or $m = 100$. As shown in Table 2, the proposed method attains essentially the same performance as the benchmark method when $m = 100$. However, the proposed method achieves a much better accuracy when $m = 20$ in terms of both the standard deviation and KL divergence.

Table 2: Estimations of the output standard deviation and KL divergence using the benchmark method and the proposed method based on 50 simulation runs. Each simulation run uses $m = 20$ or $m = 100$. The relative errors are calculated based on $\sigma_y = 2.169$, where it is estimated based on a Monte Carlo estimator with 100 simulation runs, each of which uses 10^5 random observations. The proposed method shows a better estimation accuracy than the benchmark method when $m = 20$.

Sample size	Method	Estimation	Relative error	KL divergence
20	Benchmark method	2901.137 ± 2899.45	> 100%	∞
	Proposed method	2.039 ± 0.059	5.99%	0.113 ± 0.008
100	Benchmark method	2.156 ± 0.029	0.61%	0.018 ± 0.002
	Proposed method	2.156 ± 0.029	0.61%	0.018 ± 0.003

4.4. HIV model

The HIV model used in [33] is considered as our fourth example to validate the proposed method. The output of interest is the basic reproduction number (R_0), which is arguably regarded as the most important quantity that measures the effectiveness of an infectious disease spreading through a population [34, 35]. R_0 is modeled using a deterministic equation as follows:

$$R_0 = \frac{\beta_0(1 - \gamma)\theta_d^2 + \beta_1 n_1 Q_0(n_d - \kappa) + \beta_2 n_2 \alpha Q_0 + (1 - \gamma)(\kappa + \alpha)\beta_0 \theta_d}{\theta_d(\theta_d + \kappa)(\theta_d + \alpha)}, \quad (17)$$

where the inputs follow uniform distributions with the parameters listed in Table 3. In addition, there exist correlations between β_1 and n_1 as well as between β_2 and n_2 , where the Pearson correlation coefficients are $\rho_{\beta_1, n_1} = 0.3$ and $\rho_{\beta_2, n_2} = 0.5$, respectively.

Table 3: Input descriptions and distributions of the HIV model.

Input	Descriptions	Distribution
Q_0	Recruitment rate	$U(0.0261, 0.0319)$
β_0	Birth rate of infective	$U(0.027, 0.033)$
γ	Fraction of susceptible newborn from infective class	$U(0.36, 0.44)$
β_1	Contact rate of susceptible with asymptomatic infective	$U(0.18, 0.22)$
β_2	Contact rate of susceptible with symptomatic infective	$U(0.072, 0.088)$
n_1	Number of sexual partners of susceptible with asymptomatic infective	$U(1.8, 2.2)$
n_2	Number of sexual partners of susceptible with symptomatic infective	$U(1.8, 2.2)$
θ_d	Natural death rate	$U(0.018, 0.022)$
α	Removal rate of symptomatic class	$U(0.54, 0.66)$
κ	Rate of development to AIDs	$U(0.09, 0.11)$

In this example, we set $p = 4$ for both the benchmark method and the proposed method. The benchmark method requires at least 2,000 random observations for the 10 random inputs to keep the orthogonality of the constructed orthonormal polynomials using the modified Gram-Schmidt algorithm. The lack of orthogonality of the constructed orthonormal polynomials causes inaccurate estimation, as shown in Table 4 for $m=200$. However, the proposed method still achieves accurate estimation for the same sample size. This also reflects the fact that the proposed method reduces the number of random observations

to construct a sparse PCE for models with dependent inputs. In addition, the KL divergence shown in Table 4 suggests that the proposed method has a much better performance on modeling the relationship between the input and the output.

Table 4: Estimations of the output standard deviation and KL divergence using the benchmark method and the proposed method across 50 simulation runs. Each simulation run uses a $m = 200$. The relative errors are calculated based on the theoretical value $\sigma_Y = 0.252$ provided in [33]. The proposed method provides more accurate estimation than the benchmark method.

Method	Sample size	Estimation	Relative error	KL divergence
Benchmark method	200	1034.934 ± 585.089	> 100%	∞
Proposed method		0.258 ± 0.002	2.33%	0.013 ± 0.002

5. Conclusion and future work

In this paper, we propose a data-driven sparse PCE for models with dependent inputs without requiring any distributional information about the inputs or a large number of random observations. Four numerical examples are used to validate the proposed method. It is shown that the proposed method accurately estimates the standard deviation and distribution of the output using a small sample size and improves upon the computational efficiency of the benchmark method for constructing a sparse PCE.

A recent work [20] provides interpretable sensitivity indices for models with dependent inputs without assuming the distributions or dependence structures of the inputs. This suggests a future research direction on estimating the sensitivity indices proposed in [20] using the proposed sparse PCE. In addition, the proposed method has limitations in searching all possible thresholds. Coming up with a way to efficiently find the threshold for the proposed method (analogous to the LARS algorithm for fitting all possible LASSO models on data) is a future research direction.

References

- [1] A. Avdonin, S. Jaensch, C. F. Silva, M. Češnovar, W. Polifke, Uncertainty quantification and sensitivity analysis of thermoacoustic stability with non-intrusive polynomial chaos expansion, *Combustion and Flame* 189 (2018) 300–310.
- [2] P. C. Chen, V. Malbasa, Y. Dong, M. Kezunovic, Sensitivity analysis of voltage sag based fault location with distributed generation, *IEEE Transactions on Smart Grid* 6 (4) (2015) 2098–2106.
- [3] X. Xie, R. Schenkendorf, U. Krewer, Efficient sensitivity analysis and interpretation of parameter correlations in chemical engineering, *Reliability Engineering & System Safety* 187 (2019) 159–173.
- [4] P. S. Palar, L. R. Zuhail, K. Shimoyama, T. Tsuchiya, Global sensitivity analysis via multi-fidelity polynomial chaos expansion, *Reliability Engineering & System Safety* 170 (2018) 175–190.
- [5] G. Deman, K. Konakli, B. Sudret, J. Kerrou, P. Perrochet, H. Benabderrahmane, Using sparse polynomial chaos expansions for the global sensitivity analysis of groundwater lifetime expectancy in a multi-layered hydrogeological model, *Reliability Engineering & System Safety* 147 (2016) 156–169.
- [6] J. Xu, D. Wang, Structural reliability analysis based on polynomial chaos, voronoi cells and dimension reduction technique, *Reliability Engineering & System Safety* 185 (2019) 329–340.
- [7] R. Schöbi, B. Sudret, Global sensitivity analysis in the context of imprecise probabilities (p-boxes) using sparse polynomial chaos expansions, *Reliability Engineering & System Safety* 187 (2019) 129–141.
- [8] P. Prempraneerach, F. S. Hover, M. S. Triantafyllou, G. E. Karniadakis, Uncertainty quantification in simulations of power systems: Multi-element polynomial chaos methods, *Reliability Engineering & System Safety* 95 (6) (2010) 632–646.

- [9] Z. Liu, A. G. Banerjee, Y. Choe, Identifying the influential inputs for network output variance using sparse polynomial chaos expansion, *IEEE Transactions on Automation Science and Engineering* (2020).
- [10] L. Hawchar, C.-P. El Soueidy, F. Schoefs, Principal component analysis and polynomial chaos expansion for time-variant reliability problems, *Reliability Engineering & System Safety* 167 (2017) 406–416.
- [11] N. Wiener, The homogeneous chaos, *American Journal of Mathematics* 60 (4) (1938) 897–936.
- [12] D. Xiu, G. E. Karniadakis, The Wiener–Askey polynomial chaos for stochastic differential equations, *SIAM Journal on Scientific Computing* 24 (2) (2002) 619–644.
- [13] X. Wan, G. E. Karniadakis, Multi-element generalized polynomial chaos for arbitrary probability measures, *SIAM Journal on Scientific Computing* 28 (3) (2006) 901–928.
- [14] S. Oladyshkin, W. Nowak, Data-driven uncertainty quantification using the arbitrary polynomial chaos expansion, *Reliability Engineering & System Safety* 106 (2012) 179–190.
- [15] K. Cheng, Z. Lu, Adaptive sparse polynomial chaos expansions for global sensitivity analysis based on support vector regression, *Computers & Structures* 194 (2018) 86–96.
- [16] J. A. Witteveen, S. Sarkar, H. Bijl, Modeling physical uncertainties in dynamic stall induced fluid–structure interaction of turbine blades using arbitrary polynomial chaos, *Computers & Structures* 85 (11) (2007) 866–878.
- [17] E. Torre, S. Marelli, P. Embrechts, B. Sudret, Data-driven polynomial chaos expansion for machine learning regression, *Journal of Computational Physics* 388 (2019) 601–623.

- [18] R. H. Cameron, W. T. Martin, The orthogonal development of non-linear functionals in series of Fourier-Hermite functionals, *Annals of Mathematics* (1947) 385–392.
- [19] M. P. Pettersson, G. Iaccarino, J. Nordström, *Polynomial chaos methods for hyperbolic partial differential equations*, Springer, 2015.
- [20] Z. Liu, Y. Choe, Data-driven sensitivity indices for models with dependent inputs using the polynomial chaos expansion, *Structural Safety* 88 (101984) (2021) 1–10.
- [21] L. Giraud, J. Langou, M. Rozložník, J. van den Eshof, Rounding error analysis of the classical gram-schmidt orthogonalization process, *Numerische Mathematik* 101 (1) (2005) 87–100.
- [22] G. Blatman, B. Sudret, Sparse polynomial chaos expansions and adaptive stochastic finite elements using a regression approach, *Comptes Rendus Mécanique* 336 (6) (2008) 518–523.
- [23] K. Cheng, Z. Lu, Sparse polynomial chaos expansion based on d-morph regression, *Applied Mathematics and Computation* 323 (2018) 17–30.
- [24] J. D. Jakeman, M. S. Eldred, K. Sargsyan, Enhancing l1-minimization estimates of polynomial chaos expansions using basis selection, *Journal of Computational Physics* 289 (2015) 18–34.
- [25] L. Guo, A. Narayan, T. Zhou, A gradient enhanced l1-minimization for sparse approximation of polynomial chaos expansions, *Journal of Computational Physics* 367 (2018) 49–64.
- [26] Y. Zhou, Z. Lu, W. Yun, Active sparse polynomial chaos expansion for system reliability analysis, *Reliability Engineering & System Safety* (2020) 107025.
- [27] G. Blatman, B. Sudret, Efficient computation of global sensitivity indices using sparse polynomial chaos expansions, *Reliability Engineering & System Safety* 95 (11) (2010) 1216–1229.

- [28] Q. Pan, D. Dias, Sliced inverse regression-based sparse polynomial chaos expansions for reliability analysis in high dimensions, *Reliability Engineering & System Safety* 167 (2017) 484–493.
- [29] H. Lim, L. Manuel, Distribution-free polynomial chaos expansion surrogate models for efficient structural reliability analysis, *Reliability Engineering & System Safety* 205 (2021) 107256.
- [30] S. Boltz, E. Debreuve, M. Barlaud, High-dimensional statistical measure for region-of-interest tracking, *IEEE Transactions on Image Processing* 18 (6) (2009) 1266–1283.
- [31] T. Ishigami, T. Homma, An importance quantification technique in uncertainty analysis for computer models, in: [1990] Proceedings. First International Symposium on Uncertainty Modeling and Analysis, IEEE, 1990, pp. 398–403.
- [32] S. H. Lee, B. M. Kwak, Response surface augmented moment method for efficient reliability analysis, *Structural Safety* 28 (3) (2006) 261–272.
- [33] Y. Zhu, Q. A. Wang, W. Li, X. Cai, Analytic uncertainty and sensitivity analysis of models with input correlations, *Physica A: Statistical Mechanics and its Applications* 494 (2018) 140–162.
- [34] C. Fraser, C. A. Donnelly, S. Cauchemez, W. P. Hanage, M. D. Van Kerkhove, T. D. Hollingsworth, J. Griffin, R. F. Baggaley, H. E. Jenkins, E. J. Lyons, et al., Pandemic potential of a strain of influenza A (H1N1): early findings, *Science* 324 (5934) (2009) 1557–1561.
- [35] P. Holme, N. Masuda, The basic reproduction number as a predictor for epidemic outbreaks in temporal networks, *PLOS One* 10 (3) (2015).